3. SITE 732[1]

Shipboard Scientific Party[2]

HOLE 732A

Date occupied: 25 October 1987

Date departed: 27 October 1987

Time on hole: 54 hr

Position: 32°32.81′S, 57°03.289′E

Bottom felt (rig floor; m, drill pipe measurement): 4893.0

Distance between rig floor and sea level (m): 11.10

Water depth (drill pipe measurement from sea level, m): 4881.9

Total depth (rig floor, m): 4896.00

Penetration (m): 3.00

Number of cores (including cores with no recovery): 1

Total length of cored section (m): 3.00

Total core recovered (m): 0.01

Core recovery (%): 0.3

Hard rock:
Depth (mbsf): not known
Nature: Mylonitized serpentinite

HOLE 732B

Date occupied: 27 October 1987

Date departed: 28 October 1987

Time on hole: 10 hr

Position: 32°32.81′S, 57°03.289′E

Bottom felt (rig floor; m, drill pipe measurement): 4889.4

Distance between rig floor and sea level (m): 11.10

Water depth (drill pipe measurement from sea level, m): 4878.3

Total depth (rig floor, m): 4897.40

Penetration (m): 8.00

Number of cores (including cores with no recovery): 1

Total length of cored section (m): 8.00

Total core recovered (m): 1.90

Core recovery (%): 23.8

Oldest sediment cored:
Depth (mbsf): 1.35
Nature: Volcanic sand/gravel, muddy siliceous ooze, and clasts of oceanic rocks
Earliest age: Holocene

Hard rock:
Depth (mbsf): not known
Nature: Clasts of oceanic rocks

[1] Robinson, P. T., Von Herzen, R. P., et al., 1989. *Proc. ODP, Init. Repts.*, 118: College Station, TX (Ocean Drilling Program).
[2] Shipboard Scientific Party is as given in List of Participants preceding the contents.

HOLE 732C

Date occupied: 28 October 1987

Date departed: 29 October 1987

Time on hole: 24 hr

Position: 32°32.81′S, 57°03.289′E

Bottom felt (rig floor; m, drill pipe measurement): 4896.5

Distance between rig floor and sea level (m): 11.10

Water depth (drill pipe measurement from sea level, m): 4885.4

Total depth (rig floor, m): 4920.50

Penetration (m): 24.00

Number of cores (including cores with no recovery): 3

Total length of cored section (m): 29.00

Total core recovered (m): 0.70

Core recovery (%): 2.4

Hard rock:
Depth (mbsf): not known
Nature: Basalt, gabbro, and lithic sandstone rubble

HOLE 732D

Date occupied: 29 October 1987

Date departed: 30 October 1987

Time on hole: 22 hr 45 min

Position: 32°32.85′S, 57°02.70′E

Bottom felt (rig floor; m, drill pipe measurement): 4821.0

Distance between rig floor and sea level (m): 11.10

Water depth (drill pipe measurement from sea level, m): 4809.9

Total depth (rig floor, m): 4832.00

Penetration (m): 11.00

Number of cores (including cores with no recovery): 1

Total length of cored section (m): 6.00

Total core recovered (m): 0.31

Core recovery (%): 5.2

Hard Rock:
Depth (mbsf): not known
Nature: Basalt, diabase, gabbro, and peridotite rubble

HOLE 732E

Date occupied: 30 October 1987

Date departed: 30 October 1987

Time on hole: 14 hr 45 min

Position: 32°32.85′S, 57°02.70′E

Bottom felt (rig floor; m, drill pipe measurement): 4819.0

Distance between rig floor and sea level (m): 11.10

Water depth (drill pipe measurement from sea level, m): 4807.9

Total depth (rig floor, m): 4826.00

Penetration (m): 7.00

Number of cores (including cores with no recovery): 1

Total length of cored section (m): 7.00

Total core recovered (m): 0.18

Core recovery (%): 2.6

Hard Rock:
Depth (mbsf): 5.00
Nature: Basalt and diabase rubble

HOLE 732F

Date occupied: 30 October 1987

Date departed: 31 October 1987

Time on hole: 16 hr 30 min

Position: 32°32.85′S, 57°02.70′E

Bottom felt (rig floor; m, drill pipe measurement): 4818.0

Distance between rig floor and sea level (m): 11.10

Water depth (drill pipe measurement from sea level, m): 4806.9

Total depth (rig floor, m): 4833.80

Penetration (m): 15.80

Number of cores (including cores with no recovery): 1

Total length of cored section (m): 15.80

Total core recovered (m): 0.30

Core recovery (%): 1.9

Hard rock:
Depth (mbsf): not known
Nature: Basalt and diabase rubble

Principal results: Site 732 is located on a median tectonic ridge that bisects the northern half of the north-south trending Atlantis II Transform in the Indian Ocean. Using dredge hauls from the wall of this ridge, we recovered mainly serpentinized peridotite, which suggests that the feature is a mantle diapir. The principal scientific objectives for drilling this site were (1) to determine the nature and vertical variability of rock in the median ridge, (2) to investigate the deformation of mantle rocks on the floor of the transform, (3) to determine the thermal structure of the mantle section and assess the extent of hydrothermal alteration, and (4) to determine the physical properties, magnetism, and seismic velocities of mantle rock. To achieve these objectives, we planned to drill a deep reentry hole at this site using the bare-rock guidebase.

JOIDES Resolution arrived at Site 732 at 1030 hr on 25 October 1987. We conducted a 26-hr television/sonar survey to locate areas for test spud-in and for possible guidebase deployment. The survey revealed a relatively flat, sedimented surface on top of the ridge, with some areas of rock outcrop and boulders on steep, probably faulted, flank slopes.

Six test holes were drilled in two locations at Site 732: Holes 732A through 732C at 32°32.81′S, 57°03.289′E in 4878.3 to 4885.4 m of water, determined as pipe length from rig floor minus 11.1 m (distance between the rig floor and sea level) near the break of slope, and Holes 732D through 732F at 32°32.85′S, 57°02.7′E in 4806.9 m to 4809.9 m of water nearer the ridge crest. The deepest penetration was 24 meters below seafloor (mbsf) in Hole 732C. We recovered a total of 3.51 m of material that consisted entirely of unconsolidated lithic gravel interlayered with indurated sandstone and poorly consolidated sand and muddy siliceous ooze. The siliceous ooze consists of about 60% siliceous microfossils, 35% clay, and 5% broken foraminifers. Most of the unconsolidated sand consists of volcanic detritus, including rock fragments, plagioclase, and pyroxene; the remaining part is composed of broken foraminifers and siliceous debris.

Pebbles and cobbles in the gravel range from less than 1 cm to 6 cm in maximum dimension and are subangular in shape. They consist of plagioclase phyric basalt, aphyric basalt, metabasalt, diabase, greenstone, pyroxene gabbro, metagabbro, ferrogabbro, serpentinite, serpentinized peridotite, mylonite, amphibolite, and sedimentary rock. Basalt and diabase are the most common of the recovered clasts. The clasts of sedimentary rock are small fragments of well-sorted, medium- to coarse-grained, reddish sandstone. One clast grades in size from medium to fine sand. The sand grains are angular and consist of diverse lithic and mineral fragments.

Calcareous nannofossils from the recovered sediments indicate an age of mid-Pleistocene, probably between 0.27 and 0.46 m.y. (Zone NN20). Rare specimens of reworked Miocene and Pliocene species also are present.

Drilling operations at Site 732 suggest that each hole penetrated a few (2-8) meters of soft material overlying a harder unit. Thus, the ridge appears to be capped by a poorly sorted gravel or conglomerate interlayered with sand and sandstone and overlain by a thin pelagic cover. Clasts from the gravels are similar in size and composition to those recovered from gravels on the floor of the transform during the site survey. These deposits probably were laid down by debris flows and turbidity currents that originated on the steep walls of the transform. The appearance of these basinal sediments on top of the median ridge suggests recent uplift of that feature, either by faulting or by serpentinite intrusion.

Unstable hole conditions made it impossible to reach basement at this site. Consequently, the site was abandoned and the ship moved to Site 733 on the west wall of the transform.

BACKGROUND AND SCIENTIFIC OBJECTIVES

Fracture zones are ubiquitous features of the oceanic lithosphere, yet little is known about their petrology, structure, or tectonic evolution. Recent models for fracture zones (e.g., Schouten and Klitgord, 1982) suggest that they are relatively cold zones separating stationary spreading-center cells beneath spreading-ridge segments. Crustal magma chambers are believed to lie beneath the spreading cells, with new crust being formed by crystallization on the walls of the magma chambers and by vertical and lateral dike injection along the ridge axis. In this model, less magma will reach the far edges of the spreading cells (i.e., fracture zones), leading to thinner crustal sections. Such thinning of oceanic crust in the vicinity of fracture zones has been demonstrated by seismic studies along several ridge axes (e.g., Detrick and Purdy, 1980; Fox et al., 1980; Cormier et al., 1984). In some cases, the crustal thickness in fracture zones may be less than 5% to 10% of normal sections.

Because of these relatively thin crustal sections and the great topographic relief of many fracture zones, mantle material is commonly exposed on the floors and walls of these zones. The abundance of mantle rocks in fracture zones appears to correlate closely with the spreading rate of the associated ridge. For example, peridotites make up more than 65% of all material dredged from fracture zones of the slow-spreading Southwest Indian Ridge, whereas they make up only 10%–15% of dredge hauls from fracture zones of typical slow-spreading ridges and are nearly absent from those of the fast-spreading East Pacific Rise (H. Dick, unpubl. data). Considering the difficulty of achieving deep penetration in normal oceanic crust, fracture zone drilling provides one of the best possibilities for obtaining *in-situ* samples and stratigraphy of oceanic crust and mantle.

A prime objective of Leg 118 was to penetrate and recover a deep section of mantle peridotite from the floor of the Atlantis II Fracture Zone on the Southwest Indian Ridge. A site survey conducted in October 1986 (*Conrad* cruise 27-09, H. Dick, Chief Scientist) identified a "median tectonic ridge" that bisects the northern half of the transform valley. Seismic profiles failed to locate any sediments on the ridge, and dredge hauls from the ridge flanks yielded chiefly peridotite and lesser amounts of gabbro, basalt, and greenstone. This feature appeared to be a diapiric structure along which mantle peridotite was exposed on the seafloor. Relatively flat topography on the crest of the ridge suggested that a hard-rock guidebase could be successfully deployed and used to drill a deep basement hole. Site 732 is located near the crest of this ridge, where dredge hauls recovered abundant peridotite. Major objectives of the site were as follows:

1. To determine the nature and vertical variability of rock in the median tectonic ridge.
2. To investigate the nature and extent of deformation in mantle rocks beneath the floor of the transform.
3. To determine the thermal structure of the mantle section and to assess the extent of alteration and seawater penetration.
4. To determine the physical properties, magnetism, and seismic velocities of mantle rock beneath the transform floor.

GEOLOGIC AND TECTONIC SETTING

The Atlantis II Fracture Zone trends nearly north-south and offsets the Southwest Indian Ridge at approximately 57°E (Fig. 1). The transform is about 210 km long and 30–40 km wide, as measured between the slope breaks from normal ridge topography to the steep transform walls. The spreading rate, as determined from the magnetic anomalies mapped east and west of the transform, has been about 10 mm/yr over the last 20 m.y. The magnetic anomalies created since anomaly 5 appear to extend into the transform valley near the inferred modern slip zone (Fig. 2).

Relief on the transform valley is on the order of 5800 m, and the walls of the transform valley are remarkably steep (typically 30°–40°), although locally these may be much more subdued. In detail at some locations, the walls of the transform commonly are scalloped in plan, probably because of extensive slumping and landsliding.

A bathymetrically prominent median tectonic ridge bisects the northern half of the transform valley and can be followed intermittently down the southern half as well (Fig. 3). In the north, this ridge shoals to 4200 m and has relief between 1000 and 1500 m, whereas in the southern half of the valley the relief drops abruptly to only a few hundred meters. From four dredge hauls along the median tectonic ridge chiefly serpentinized peridotite and lesser amounts of gabbro, metamorphosed basalt, and diabase were recovered. Virtually all of the basaltic rocks recovered have been altered, and this alteration was usually oxidative, with many of the rocks stained a bright red or white. In addition, some unusual breccias cemented by a black tarry-appearing hydrothermal oxide were recovered.

The position of the median tectonic ridge suggests that it marks today's slip boundary in the transform. We believe it is composed chiefly of peridotite, perhaps in the form of a mantle diapir. The nature of the altered rocks suggests that the conditions of hydrothermal alteration along the transform plate boundary may differ substantially from those occurring along ocean ridges.

OPERATIONS

Port Louis Port Call

Leg 118 commenced in Port Louis, Mauritius, at 0700 hr, 18 October 1987, when *JOIDES Resolution* dropped anchor in the Port Louis harbor. (All times are local ship time unless stated otherwise.) ODP personnel boarded the ship during the morning, the Schlumberger cable was changed, and inspection of the drill pipe began. At 2145 hr on 19 October 1987, the ship shifted to the dock, and fuel and air cargo were taken aboard. During 20 and 21 October 1987, sea freight was loaded on the ship, while surplus equipment was offloaded to make room for the hard-rock guidebase and a large quantity of ancillary hard-rock drilling equipment. By the morning of 22 October 1987, all drill pipe used since the last inspection had been inspected, and the ship got under way at 1200 hr on 22 October 1987.

Approach to Site 732

The general location for Site 732 was selected on the median ridge of the Atlantis II Transform (Fig. 3), based on contoured Sea Beam bathymetric maps and a dredge haul that recovered peridotite almost exclusively. A small area at this location was selected for detailed surveying before dropping the beacon. The track of the ship from Mauritius was planned to minimize the time necessary to reach that location.

The voyage to the median ridge was uneventful, and at 0900 hr on 25 October 1987 the ship slowed to begin the site survey. A voyage of 771 nmi was made in 71.5 hr at an average speed of 10.8 kt. We planned for an initial brief survey to establish the exact location of the Sea Beam bathymetric contours using the global positioning system (GPS) navigating equipment aboard the ship. Although the Sea Beam mapping had also been controlled by GPS and transit satellite navigation, we thought that parts of track lines between navigation control might be off the location by 1 to 2 nmi.

The final track lines of the echo sounding survey (Fig. 4) closely reproduced the planned track, which was designed based on trends of the Sea Beam contours. We planned for the beacon to be located directly upslope of the dredge haul on the east flank of the median ridge, and the track lines were laid out to cross in nearly orthogonal direction to the north-south trending depth contours of the median ridge. The survey lines extended from the adjacent eastern basin floor across the crest of the ridge. Because the depth contours were strongly aligned in a north-south direction, control of contour location was best in the east-west direction. Fortunately, the ship arrived for the beacon survey during GPS coverage, which resulted in an efficient survey. The depths expected from the Sea Beam maps were well reproduced along the ship's track. Apparently, the map contours were accurately located in this region, at least in the east-west direction.

Although the ship's standard echo sounders (12 and 3.5 kHz) were operated, very little data were recorded at normal ship speed (10 to 12 kt) because of the high background noise of the ship. Hence, the ship was slowed to about 6 kt before arriving at the first turning point of the survey. The most useful recordings (Fig. 5) were obtained with the seismic profiling system (single channel, water-gun source) towed astern. The beacon was dropped at the end of the survey (1030 hr, 25 October 1987), based on the planned GPS location, and landed just east of the median ridge summit at 32°32.75′S, 57°03.10′E at a water depth of about 4800 m.

Television/Sonar Survey

After dropping the beacon, we began a survey with the television/sonar system suspended on the coaxial cable through the moon pool (without pipe). Offsets of the ship from the bottom beacon and from a beacon on the camera frame were recorded during the survey and used to calculate the offsets of the camera from the bottom reference beacon (Fig. 6). Visual impressions of the bottom character recorded on videotape and in writing were used to prepare an annotated map of relevant features on the seafloor. The amount of wire played out was also recorded as an indication of depth, and a ball 0.3 m in diameter was suspended about 10 m below the camera frame to provide a useful scale for bottom features and to indicate height above bottom to the winch operator.

The survey lines were run in an "E" pattern, with one irregular north-south profile nearly 4 km long near the crest of the ridge and three other profiles intersecting it orthogonally (each about 2 km long) down the east slope. Survey tracks were run downslope where appropriate to avoid catching the camera frame on cliffs or large boulders. The survey was performed from

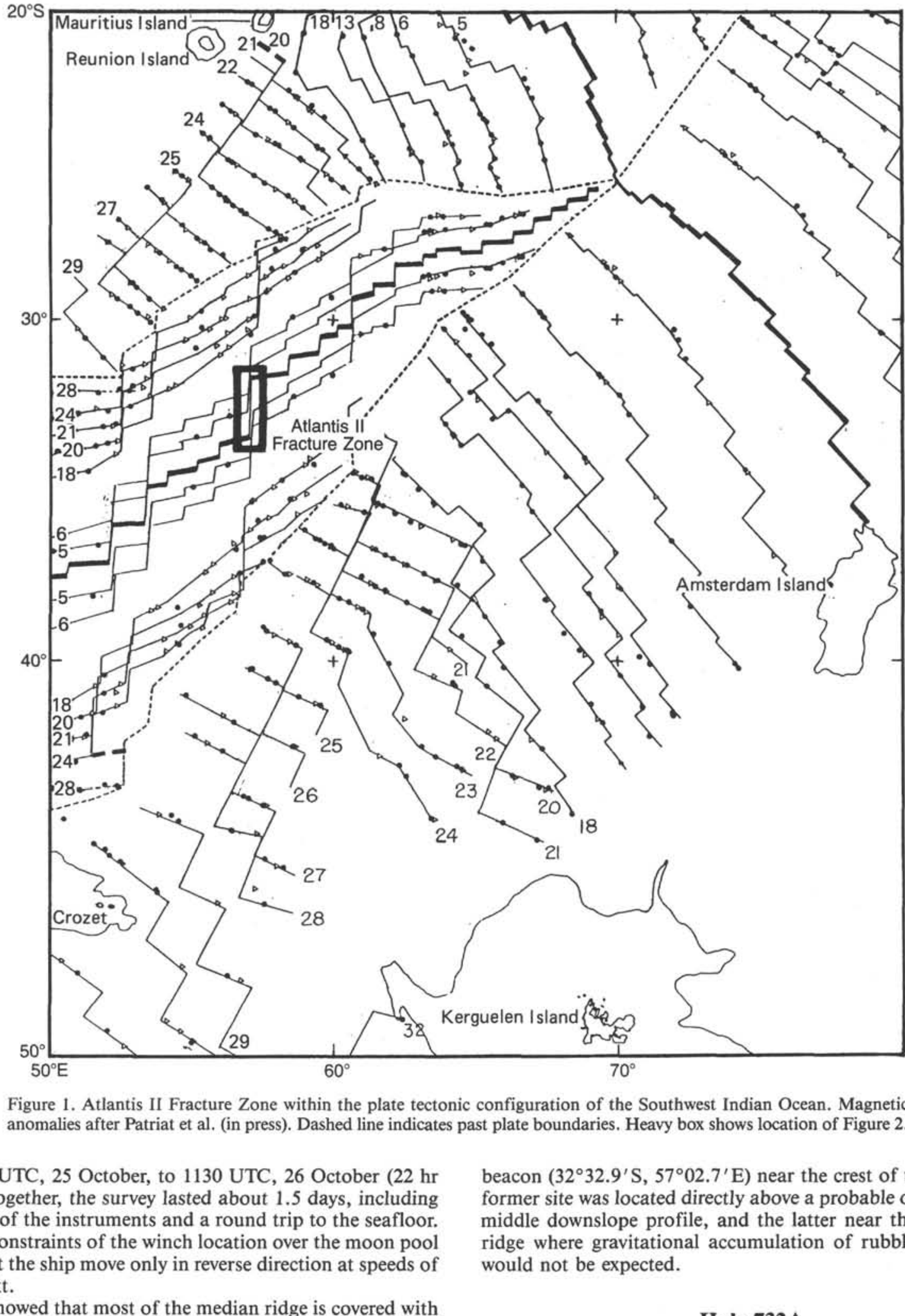

Figure 1. Atlantis II Fracture Zone within the plate tectonic configuration of the Southwest Indian Ocean. Magnetic anomalies after Patriat et al. (in press). Dashed line indicates past plate boundaries. Heavy box shows location of Figure 2.

about 1345 UTC, 25 October, to 1130 UTC, 26 October (22 hr 45 min); altogether, the survey lasted about 1.5 days, including preparation of the instruments and a round trip to the seafloor. Geometric constraints of the winch location over the moon pool required that the ship move only in reverse direction at speeds of 1/2 to 2/3 kt.

Results showed that most of the median ridge is covered with sediment and/or rubble of unknown thickness, with a few large blocks or boulders (one to several meters in dimensions) on or near steep slopes. We had difficulty determining whether some of the larger sized material was outcrop or had been displaced. Two sites within the survey region were selected for spud-in attempts; each site sloped less than 20° and was large enough for guidebase deployment. One site was 500 m due east of the beacon (32°32.8′S, 57°03.3′E) and the other, 400 m west of the beacon (32°32.9′S, 57°02.7′E) near the crest of the ridge. The former site was located directly above a probable outcrop on the middle downslope profile, and the latter near the crest of the ridge where gravitational accumulation of rubble from above would not be expected.

Hole 732A

The operational plan was to test drill the site before committing the hard-rock guidebase. Test drilling should determine whether a hole could be started in hard rock using an unsupported bottom-hole assembly (BHA). The BHA consisted of a 10½ in. bit (RBI C4), crossover sub, a coring motor, five 8¼ in. drill collars, crossover sub, one 7¼ in. drill collar, and six stands of 5¼ in. drill pipe.

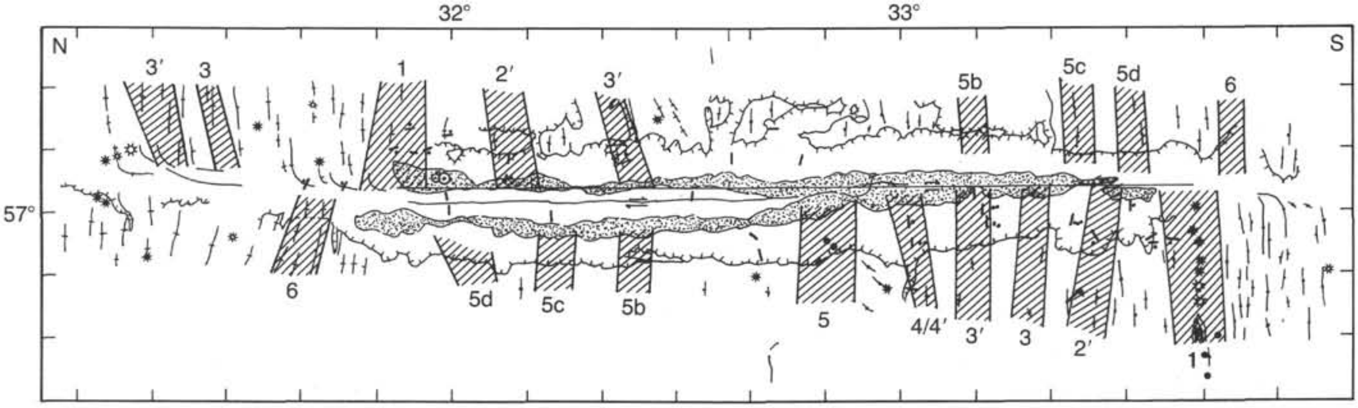

Figure 2. Tectonic map of the Atlantis II Fracture Zone (after Dick et al., unpubl. data). Hatched linear zones are preliminary magnetic anomaly identifications. Short lines and circles are rock dredge locations. Arrows highlight dredges consisting predominantly of serpentinized peridotite. Dotted areas denote basins.

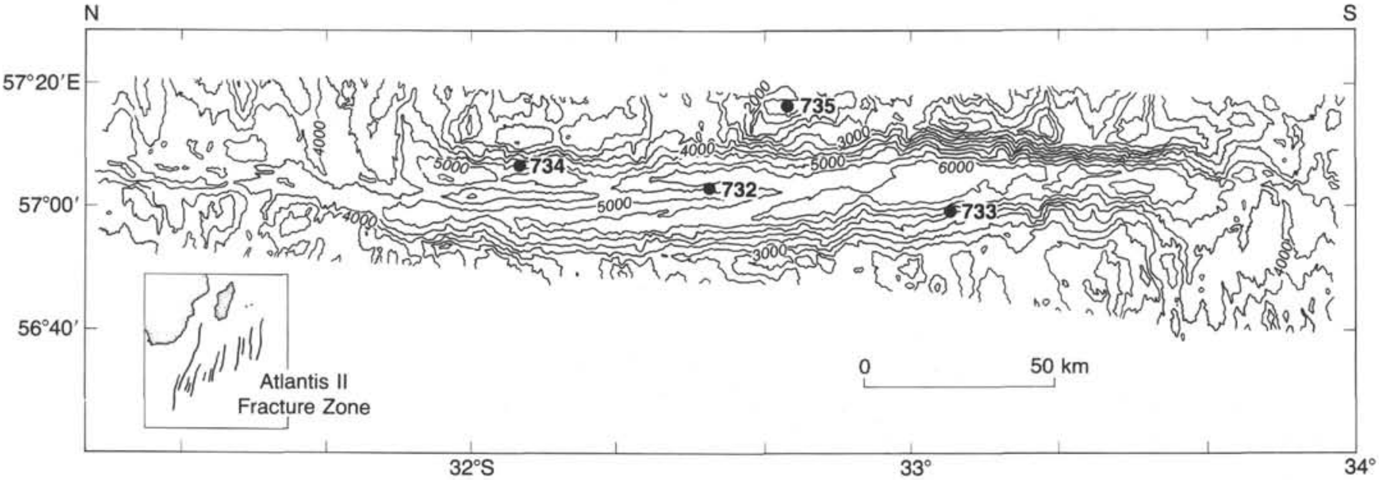

Figure 3. Bathymetric map with contours at 500-m intervals of the Atlantis II Fracture Zone, Southwest Indian Ridge, showing Leg 118 drill sites. Survey from *Conrad* cruise 27-09, 1986 (H. Dick, Chief Scientist, with D. Gallo and R. Tyce).

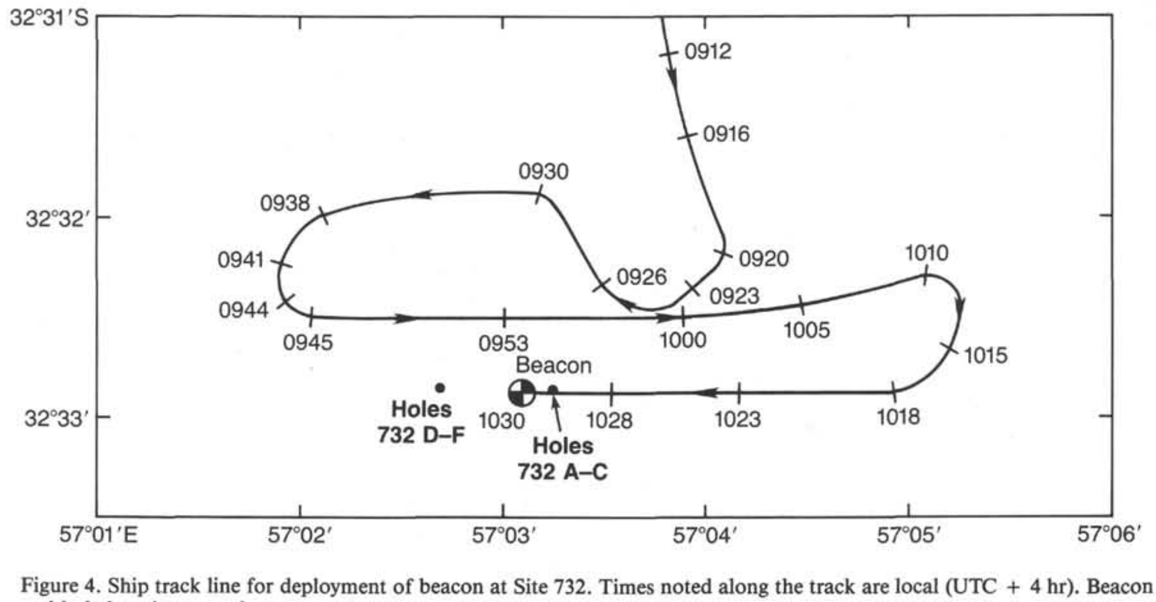

Figure 4. Ship track line for deployment of beacon at Site 732. Times noted along the track are local (UTC + 4 hr). Beacon and hole locations are shown.

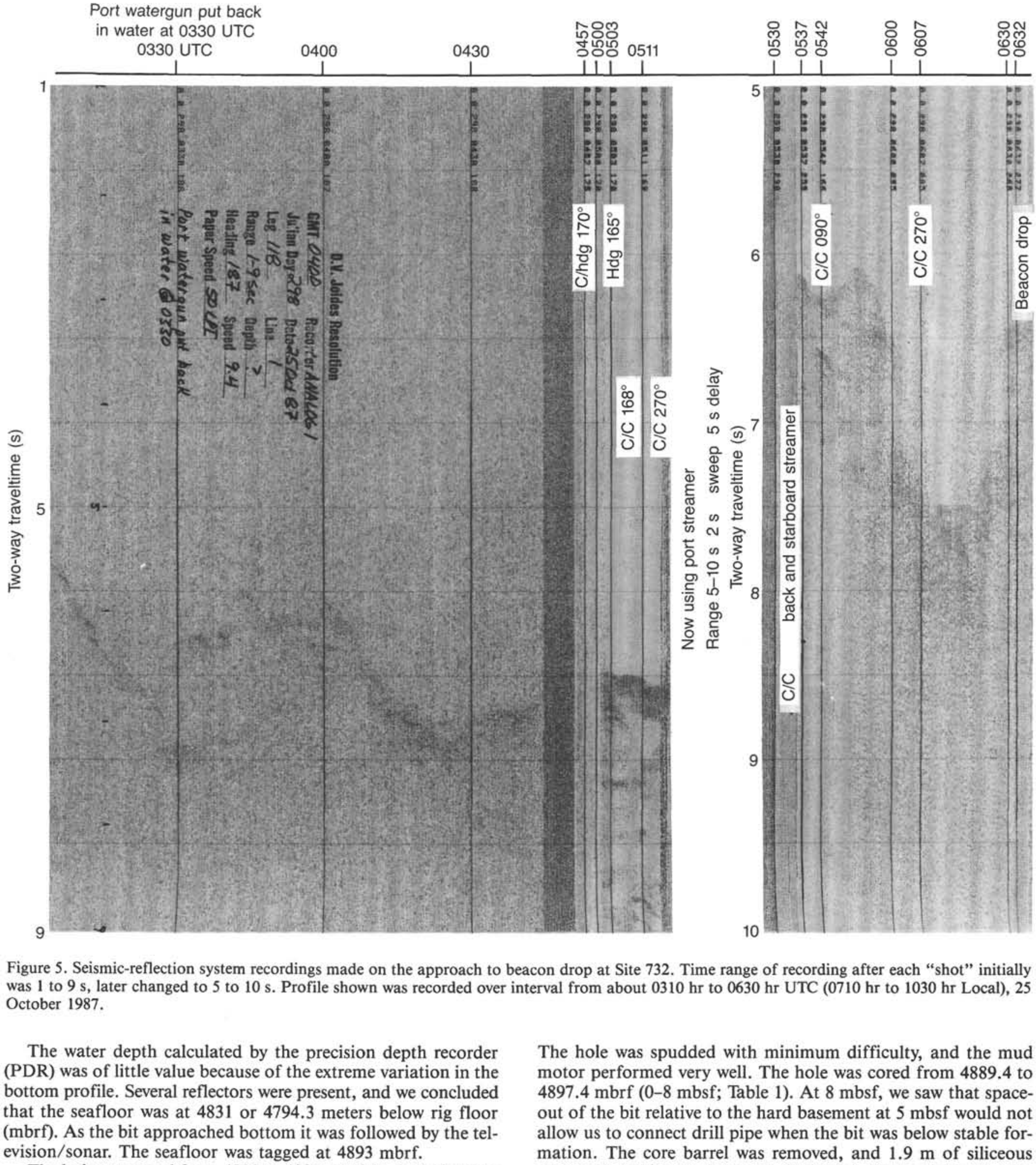

Figure 5. Seismic-reflection system recordings made on the approach to beacon drop at Site 732. Time range of recording after each "shot" initially was 1 to 9 s, later changed to 5 to 10 s. Profile shown was recorded over interval from about 0310 hr to 0630 hr UTC (0710 hr to 1030 hr Local), 25 October 1987.

The water depth calculated by the precision depth recorder (PDR) was of little value because of the extreme variation in the bottom profile. Several reflectors were present, and we concluded that the seafloor was at 4831 or 4794.3 meters below rig floor (mbrf). As the bit approached bottom it was followed by the television/sonar. The seafloor was tagged at 4893 mbrf.

The hole was cored from 4893 to 4896 mbrf (0–3 mbsf; Table 1), at which point a pressure leak developed in the drill-string weight indicator system. To repair the leak, we had to pull the bit above the seafloor. The core barrel was pulled to the surface, and a fragment of mylonitized serpentinite was recovered.

Hole 732B

The bit was observed on the television/sonar to penetrate about 5 m of very soft sediment before it began to take weight. The hole was spudded with minimum difficulty, and the mud motor performed very well. The hole was cored from 4889.4 to 4897.4 mbrf (0–8 mbsf; Table 1). At 8 mbsf, we saw that space-out of the bit relative to the hard basement at 5 mbsf would not allow us to connect drill pipe when the bit was below stable formation. The core barrel was removed, and 1.9 m of siliceous ooze and sand was recovered, including clasts of basalt, diabase, gabbro, and serpentinite.

Hole 732C

The hole was cored from 4896.5 to 4920.5 mbrf (0–24 mbsf; Table 1). When the bit was raised off the bottom to connect drill pipe, the hole collapsed. It was re-drilled to 4916 mbrf (19 mbsf), and several mud slugs were pumped in an effort to stabilize the walls, but more hole was lost. Because we did not know the

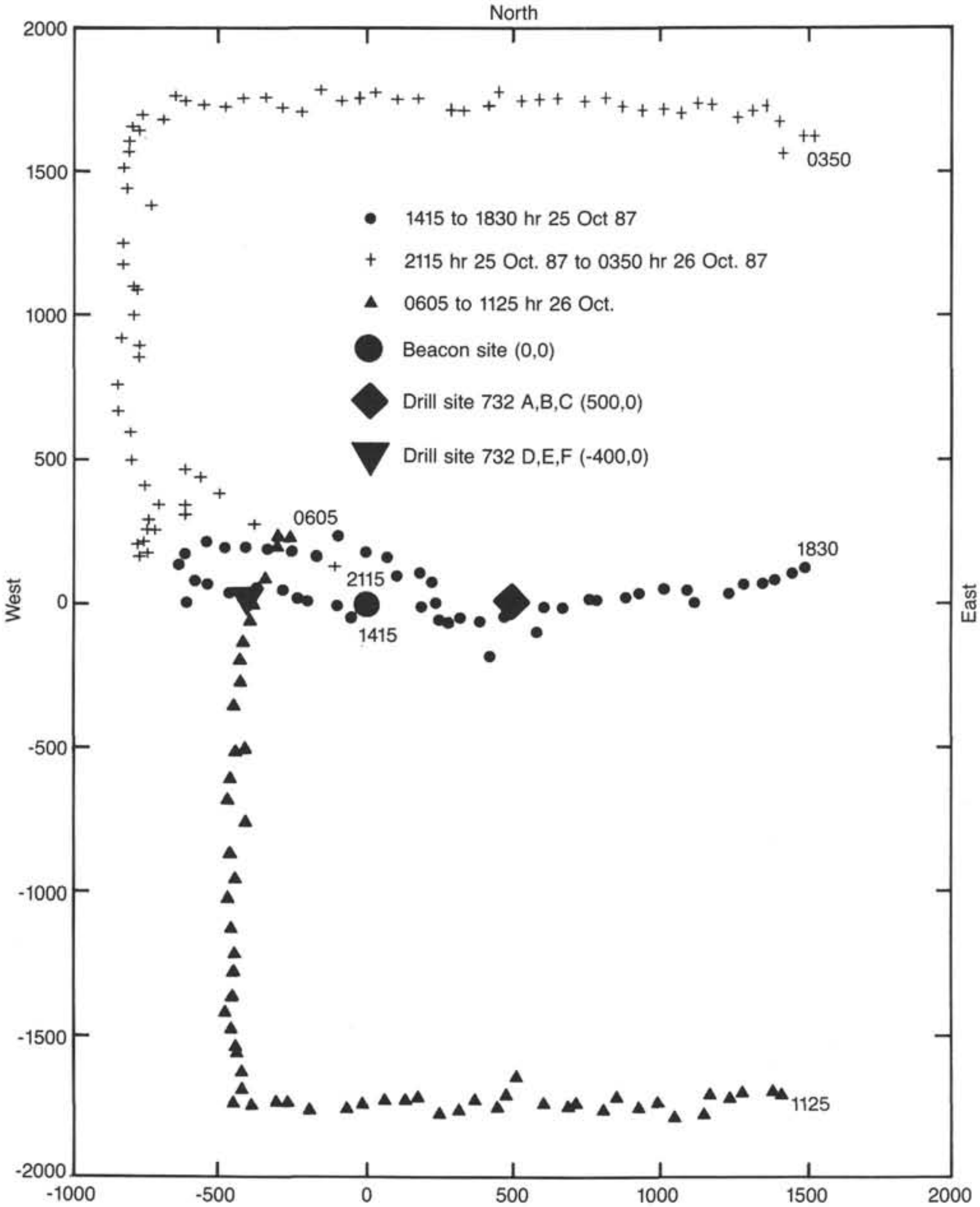

Figure 6. Plot of navigation for TV camera/sonar survey at Site 732. Symbols are positions at nominal 5-min intervals over various time periods (UTC) during survey as indicated. Beacon at origin of plot is located at 32°32.8′S, 57°03.0′E; drill-hole locations also are shown. Axis dimensions in meters from beacon.

thickness of the rubble or the bad caving conditions, we decided that coring at this site was not advisable. A total of 0.7 m of basalt, gabbro, and lithic sandstone rubble was recovered in the core barrel.

Hole 732D

The ship was moved 900 m due west of Holes 732A, 732B, and 732C, nearer to the top of the ridge, where we thought there would be less rubble. The mud line was located at 4821.0 mbrf by using the television/sonar. The bit pushed through 5 m of soft sediment (Table 1). The hole was stable, but the drilling rate was very slow. It took 5.25 hr to core 6 m to 4832.0 mbrf (11 mbsf), at which time the bit stopped drilling. The drilling rate suggested that the bit was worn out; thus, the pipe was tripped out of the hole. When the bit reached the surface, we were surprised to find that it was in nearly new condition. A total of 0.31 m of rubble composed of basalt, diabase, gabbro, and peridotite was recovered.

Hole 732E

Because of the presence of the 5-m-thick sediment cover, we concluded that spud-in with a conventional rotary core bit was possible. The advantage of the rotary system is its ruggedness and its relatively low cost compared to that of the mud motor. Not only are mud motors costly, but the only two in existence were on board the ship; their loss due to BHA failure was a concern.

The BHA consisted of the 9⅞ in. bit (an RBI C4), long bit sub, control drill collar, long top sub, head sub, seven 8¼ in. drill collars, crossover sub, one 7¼ in. drill collar, crossover

Table 1. Coring summary for Site 732.

Core	Date (Oct. 1987)	Time (Local)	Total depth[a] (mbrf)	Depth (mbsf)	Length advanced (m)	Length cored (m)	Length recovered (m)	Recovery (%)
118-732A-1D	27	17.45	4893.0–4896.0	0–3.0	3.0	3.0	0.01	0.3
732B-1D	28	01.30	4889.4–4897.4	0–8.0	8.0	8.0	1.90	23.8
732C-1D	28	08.15	4896.5–4910.5	0–14.0	14.0	14.0	0.0	0.0
732C-2D	28	17.30	4910.5–4920.5	14.0–24.0	10.0	10.0	0.35	3.5
[b]732C-3D	28	23.00	4910.5–4915.5	14.0–19.0	0.0	5.0	0.35	7.0
732D-1	29	—	4821.0–4826.0	0–5.0	5.0	0.0	0.0	—
732D-1D	29	12.30	4826.0–4832.0	5.0–11.0	6.0	6.0	0.31	5.2
732E-1R	30	14.50	4819.0–4826.0	0–7.0	7.0	7.0	0.18	2.6
732F-1R	30	20.05	4818.0–4833.8	0–15.8	15.8	15.8	0.30	1.9
[c]732F-2B	30	20.05	4818.0–4833.8	0–15.8	0.0	0.0	0.01	—

[a] Determined as pipe length from rig floor.
[b] Rubble fill.
[c] As fragments recovered from bit; not cored.

sub, and six stands of 5⅓ in. drill pipe. The bottom three drill collars were inspected for cracks; none were found.

The bit took weight at 4819 mbrf, and the hole was cored to 4826 mbrf (7 mbsf; Table 1) in 68 min. The pipe became stuck and required 150,000 lb of overpull to free it, but the combination of pipe stretch and finite response time of the motion compensator caused the pipe to rebound out of the hole. A wireline trip was made for the core barrel, and 0.18 m of basalt and diabase rubble was recovered.

Hole 732F

The ship was moved 15 m west toward the median ridge crest. The bit took weight at 4818 mbrf (Table 1). The coring rate was satisfactory, but nearly every time the bit was picked up off the bottom, the hole collapsed. At 4833.8 mbrf (15.8 mbsf), the bit was raised to 4 mbsf to recover the core barrel. A total of 0.3 m of basalt and diabase rubble was recovered. Although the hole was filled with mud, it collapsed. The bit struck bottom a couple of times during a down heave of the ship while the hole continued to collapse. The bit was pulled clear of the seafloor to protect the drill string from compressional damage.

Test spud-ins at Site 732 suggest that the median ridge is capped by at least 5 m of soft sediment overlying sand and gravel that contain boulders of considerable size and quantity. We do not know how thick this material is; it is too unstable for drilling. Hence, Site 732 was deemed unsuitable for guidebase deployment and was abandoned. The *JOIDES Resolution* departed for Site 733 at 0830 hr on 31 October 1987.

SEDIMENTOLOGY

A 135-cm-thick section of sediment was recovered from Hole 732B (Section 118-732B-1D-1) overlying 15 cm of weathered basalt pebbles. These sediments, and about 10 cm^3 of sediment scraped from the bit in Hole 732F (Core 118-732F-2B), were the only sediments recovered at Site 732. Drilling disturbance was severe throughout, and no unambiguous sedimentary structures were observed. Two lithologies are present in the upper 70 cm: (1) a very dark grayish brown, well-sorted, medium- to coarse-grained volcanogenic sand (90%), and (2) a yellow brown muddy siliceous ooze (10%). The sand consists chiefly of rock fragments and subrounded grains of plagioclase and pyroxene, with about 10% broken foraminifers and siliceous debris. The ooze contains about 60% siliceous microfossils, 35% clay, and 5% broken foraminifers.

The interval between 70 and 95 cm in Section 118-732B-1D-1 contains gravel as well as the sand and ooze described above. The gravel consists of subrounded pieces of weathered basalt and serpentinite up to 2 cm in diameter. Between 95 and 135 cm, the core contains 60% to 70% yellow brown muddy siliceous ooze, 20%-30% black basalt gravel pieces, and 10% very dark grayish brown, coarse volcanic sand.

The volcanic sand and the muddy siliceous ooze are recognized as distinct lithologies, despite severe coring disturbance. These lithologies probably represent separate modes of sedimentation. The fine grain size and large biogenic fraction of the ooze indicate that it is pelagic in origin. The coarse-grained, well-sorted character of the sand and the rounded nature of the grains suggest deposition from density currents or reworking by bottom currents. Large slump scars on the walls of the fracture zone and associated fans in the axis were identified in detailed bathymetry (H. Dick, unpubl. data). Turbidity currents originating from large-scale mass movements may have distributed both sand and gravel along the floor of the fracture zone. Alternatively, episodes of strong northward bottom-current flow (Warren, 1978) may have reworked volcanic debris on the fracture zone floor to form the well-sorted sand beds.

BIOSTRATIGRAPHY

At Site 732, sediments were recovered from Section 118-732B-1D-1 and from Core 118-732F-2B, where they were scraped off the drill bit. The sediments from Hole 732F may have come from any depth over the drilled interval of 0 to 15.8 mbsf, but probably are from near the surface. The biogenic content of the sediments was analyzed in smear slides. All samples contain abundant diatom fragments and sponge spicules. Some foraminifers, calcareous nannofossils, radiolarians, and silicoflagellates also are present. Preservation of all fossil groups is poor.

Sediments are dated as mid-Pleistocene, probably between about 0.268–0.458 Ma, based on calcareous nannofossils. The occurrence of Oligocene to Pliocene age indicators, together with distinctly Pleistocene species (the latter dominate), suggests significant reworking and/or slumping at this site.

Calcareous Nannofossils

The sediments from Hole 732F and eight smear slides from Hole 732B were examined for their content of calcareous nannofossils (Samples 118-732B-1D-1, 12, 40, 66, 85, 102, 116, 125, and 140 cm). Two samples (118-732B-1D-1, 64 and 139 cm) were also analyzed using scanning electron microscopy (SEM). Taxonomy follows Perch-Nielsen (1985), and biostratigraphic zonation is after Martini (1971).

All samples contain the same assemblage: mainly small (<4 μm) placoliths and *Calcidiscus leptoporus* and some *Coccolithus pelagicus* and ceratoliths. A few specimens of reworked Oligocene-Pliocene species also were observed (*Cyclicargolithus abisectus, Dictycoccites* sp., *Discoaster brouweri, D. variabilis, D.*

quinqueramus, *Helicosphaera sellii*, *Pseudoemiliania lacunosa*, *Reticulofenestra umbilicus*, *R. pseudoumbilicus*). Preservation is poor, and the assemblage is enriched in solution-resistant forms.

Gephyrocapsa oceanica and other *Gephyrocapsa* species are well established, but *Emiliania huxleyi* was not observed. Only two specimens of *P. lacunosa* and few *H. sellii* were observed after many hours of analysis; these probably represent reworked specimens. Thus, the sediments are tentatively assigned to Zone NN20. The last occurrence of *P. lacunosa* is estimated to have occurred at 0.458 Ma, and the first occurrence of *E. huxleyi* is estimated at about 0.268 Ma by Thierstein et al. (1977), giving the ages of the lower and upper boundaries of this zone.

LITHOSTRATIGRAPHY

The only materials recovered from the six holes drilled at Site 732 are unconsolidated lithic granules, pebbles, and cobbles interlayered with indurated sandstone, poorly consolidated sand, and tan, muddy siliceous ooze. Drilling operations suggested that in each hole a few (2–8) meters of soft material overlies a harder unit. The upper soft sediment is probably represented by the muddy siliceous ooze, and the lower unit by igneous and metamorphic breccia or conglomerate with interlayered sand and sandstone.

Siliceous ooze was recovered only in Core 118-732B-1D and from the bit in Hole 732F (Core 118-732F-2B) after the pipe was tripped. The sediment contains Quaternary and reworked Oligocene-Pliocene fauna (see "Biostratigraphy" section, this chapter). In the other cores this material probably washed out of the core barrel during drilling or in transit to the surface.

The coarse grains and clasts in the harder, lower unit range from less than 1 to 8 cm in maximum dimension and include igneous, metamorphic, and sedimentary rocks. All are subangular and have slightly rounded edges and buff to gray, weathered surfaces. All clearly are clasts in a poorly lithified deposit, not fragments produced as a consequence of drilling. Some of the igneous clasts have thin patches of indurated sand on their surfaces, indicating that they derive from a poorly sorted deposit partially cemented by iron-oxyhydroxides.

The clasts of sedimentary rock are small fragments of well-sorted, medium- to coarse-grained, reddish sandstone. One piece is graded from medium to fine sand. Grains are angular and include diverse lithic and mineral fragments. An unlithified sand interval in Core 118-732B-1D includes grains of similar size and composition.

Igneous and metamorphic clasts and very coarse grains in the breccia include plagioclase phyric basalt, aphyric basalt, metabasalt, greenstone, pyroxene gabbro, metagabbro, serpentinite, serpentinized peridotite mylonite, amphibolite gneiss, ferrogabbro, and diabase. Basalt and diabase are volumetrically the most common of the recovered clasts.

The upper part of the median ridge in the Atlantis II Fracture Zone appears to be a poorly sorted breccia or conglomerate interlayered with moderately to well-sorted immature sand and sandstone, overlain by a thin cover of pelagic sediment. The clast sizes and lithologies are similar to gravels recovered from the floor of the fracture zone east of Site 732 (H.J.B. Dick, pers. comm., 1987). These deposits are probably debris flows and turbidity deposits shed from the steep walls of the fracture zone. The cored breccia may be such basinal deposits that have been uplifted by faulting or by serpentinite intrusion along the median ridge. They could also be materials deposited from debris flows having sufficient velocity to have overwashed the median ridge.

PETROGRAPHY

Introduction

Holes 732A through 732F were spudded into an unknown thickness of clastic sediment and rubble. Approximately 3.5 m of rock and sediment was recovered from six holes, with a maximum penetration depth of 24 mbsf in Hole 732C and a maximum recovery of 23.8% in Hole 732B (Table 1). Material recovered includes a range of fresh, altered, and/or deformed mafic and ultramafic rock types. Relative proportions of all rock types recovered are listed in Table 2. For clast sizes greater than 2 cm, basalt, diabase and gabbro (in decreasing order of abundance) predominate (Table 2); ultramafic materials constitute less than 3% of the total. For clast sizes between 1 and 2 cm, however, basalt, gabbro and serpentine occur in roughly equal proportions (Table 2). This section reviews the petrography of the primary mineral assemblages; alteration and deformation of these samples are discussed in a subsequent section on alteration.

Petrography of Rubble Clasts

Basalt

Basaltic rocks range from aphyric to sparsely plagioclase or olivine phyric. Aphyric and plagioclase phyric samples predominate and occur in roughly equal proportions. Olivine phenocrysts, approximately 0.5 mm across, occur only in Sample 118-732F-1R-1, 0–4 cm, although olivine microphenocrysts (<1 mm in size) were identified in Samples 118-732C-2D-1, 14–17 cm and 118-732C-2D-1, 19–21 cm. The microphenocrysts in these samples are now totally replaced by clay minerals and calcite. Plagioclase phenocrysts range from 1 to 6 mm in size and generally make up less than 4% of the rock, although one meta-basalt fragment (Sample 118-732E-1R-1, 15–20 cm) contains approximately 25% plagioclase phenocrysts up to 3 mm in size. Plagioclase constitutes 45%–50%, clinopyroxene 5%–45%, and olivine, if present, less than 8% of the groundmass. All basalt clasts have quench crystallization textures consisting of plagioclase sheaf structures and, in some cases, lantern groundmass olivine (now totally replaced by chlorite or clay). Although groundmass textures indicate relatively rapid cooling for these basalts, no glass was recovered. Vesicles were observed in only two samples; in Sample 118-732C-2D-1, 14–17 cm, these were filled by smectite and in Sample 118-732D-1D-1, 0–5 cm, by chlorite.

Alteration consists predominantly of plagioclase replacement by chlorite, clay minerals, epidote, and/or albite. Olivine is replaced by calcite or chlorite and cryptocrystalline groundmass, by clay minerals or chlorite.

Diabase

Diabase clasts recovered from Holes 732A through 732F are predominantly fine-grained, dark to medium gray rocks. They consist of approximately 50% plagioclase, 20%–30% clinopyroxene, and 5%–10% iron and titanium oxides. Olivine, which probably constituted 10%–15% of the primary assemblage, has been totally replaced by clay minerals and iron and titanium oxides. Textures range from equigranular to subophitic.

One unusual sample, 118-732D-1D-1, 20–30 cm, has 1%–2% plagioclase phenocrysts/xenocrysts up to 1 cm in size; smaller (2 mm), less abundant iron and titanium oxide xenocrysts also occur. This sample is by a fine-grained basaltic dikelet, approximately 1 cm wide (Fig. 7). Contacts between the dikelet and host diabase are sharp, but chilled margins are not apparent. The basaltic dikelet contains plagioclase xenocrysts, probably incorpo-

Table 2. Lithologic summary for all clast types.

Rock type		Number of clasts	Percentage
Clasts < 1 cm			
Basalt		38	33.9
Gabbro		23	20.5
Serpentine		20	17.8
Diabase		17	15.2
Greenstone		5	4.5
Lithic sandstone		3	2.7
Gabbroic gneiss		2	1.8
Greenschist facies microbreccia		2	1.8
Serpentinized peridotite/mylonite		1	0.9
Serpentinized harzburgite		1	0.9
Clasts > 2 cm			
Basalt		14	45.2
aphyric	(19.4%)		
plagioclase phyric	(19.4%)		
vesicular, plagioclase phyric	(3.2%)		
olivine phyric	(3.2%)		
Diabase		8	25.8
Gabbro		3	9.7
Lithic sandstone		3	9.7
Gabbroic gneiss		1	3.2
Serpentinized peridotite/mylonite		1	3.2
Serpentinized harzburgite		1	3.2
Clasts 1-2 cm			
Weathered basalt		24	29.6
Gabbro		20	24.7
Serpentine		20	24.7
Diabase		9	11.1
Greenstone		5	6.2
Greenstone facies microbreccia		2	2.5
Gabbroic gneiss		1	1.2

Figure 7. Diabase Sample 118-732D-1D-1, 20-30 cm, with crosscutting basaltic dikelet. Basaltic dikelet extends from upper left to lower right of sample and is approximately 1 cm wide.

rated from the diabase wall rock. The dikelet exhibits significantly more oxidative alteration than the adjacent diabase.

Alteration in most diabase clasts consists of replacement of olivine and/or interstitial glass by clay minerals and minor replacement of plagioclase by clay minerals or chlorite. One diabase contains a greenschist-grade secondary mineral assemblage (see "Alteration, Metamorphism and Deformation" section, this chapter).

Gabbro

Gabbro clasts range from moderately (10%-40%) to very highly (80%-95%) altered and deformed and are probably best described as metagabbros. Structurally, they range from massive to foliated. Texturally, they range from coarse- to very coarse-grained, with plagioclase and clinopyroxene crystals up to 1 cm in size. Most samples recovered are one-pyroxene gabbros consisting of 45%-80% plagioclase, 20%-40% clinopyroxene, and less than 5% iron and titanium oxides.

Neither orthopyroxene nor olivine is believed to have been present in the primary mineral assemblages of most gabbro samples recovered, but this was difficult to assess because of the nearly complete replacement of primary minerals in most samples. However, petrographic evidence suggests that completely serpentinized porphyroclasts in Samples 118-732D-1D-1, 7-8 cm, and 118-732B-1D-2, 5-6 cm, have replaced orthopyroxene. These samples originally contained 30%-50% plagioclase, 30% clinopyroxene, 8%-10% orthopyroxene, 2%-20% iron and titanium oxides, and 10% hornblende. Sample 118-732D-1D-1, 7-8 cm, also contains traces of euhedral apatite up to 1 mm in length. The reddish-brown hornblende that surrounds cumulate ilmenite in this sample is apparently primary. In contrast to the one-pyroxene assemblages, this mineralogy suggests that these rocks are probably ferro-gabbros. Like the one-pyroxene gabbros, Sample 118-732D-1D-1, 7-8 cm, is very coarse-grained and massive. Sample 118-732B-1D-2, 5-6 cm, is a medium-grained, foliated rock, but was probably also coarse-grained originally as porphyroclasts of up to 5 mm were observed.

Ultramafic Rocks

Ultramafic rocks recovered at Site 732 consist almost exclusively of serpentinite. In Sample 118-732A-1D-1, 0-4 cm, a serpentinite mylonite peridotite, almost all evidence of primary mineralogy has been lost because of extensive alteration and deformation. However, Samples 118-732B-1D-2, 8-9 cm, and 118-732D-1D-1, 12-18 cm, are far less deformed and contain bastite pseudomorphs after pyroxene (up to 5 mm in size) and relict holly-leaf chromium-spinel. Some bastite pseudomorphs in Sample 118-732B-1D-2, 8-9 cm, also contain primary clinopyroxene having orthopyroxene exsolution lamellae. These samples probably were originally coarse-grained harzburgites.

Lithic Sandstone

Three fragments of lithic sandstone were recovered along with the various mafic and ultramafic samples from Hole 732C (118-732C-2D-1, 25-35 cm; 118-732C-2D-1, 35-39 cm; 118-732C-3D-1, 27-30 cm). Consistent with the predominant recovery of basalt among the larger clast sizes (>1 cm), the sandstones consist principally of basalt and diabase fragments (20%) and plagioclase (21%). Most basalt clasts have quench textures (i.e., plagioclase sheaf structures) similar to those described previously, as well as variolitic structures and palagonitized glass. A variety of secondary alteration minerals constitute the remainder of the rock (Table 3). The grains are cemented by a dark red opaque material, probably a ferro-manganese oxyhydroxide.

Summary

A wide variety of intrusive and extrusive rocks was recovered from the sedimentary unit cored in Holes 732A through 732F. Clasts greater than 1 to 2 cm are predominantly mafic igneous rocks (basalt, diabase, and gabbro), accompanied by lesser amounts of altered or metamorphosed equivalents and ultramafic materials.

ALTERATION, METAMORPHISM, AND DEFORMATION

Introduction

As discussed in the "Petrography" section (this chapter), the rubble samples provide a random selection of rocks from the transform fault wall. The basalts show variable degrees of low-

Table 3. Point-count summary of lithic sandstone from Sample 118-732C-2D-1, 35-39.

Clast type	Point count	Percentage
Basalt and diabase	153	20.4
Plagioclase	160	21.3
Chlorite	42	5.6
Colorless amphibole	38	5.1
Clay minerals	24	3.2
Clinopyroxene	16	2.1
Blue-green amphibole	5	0.7
Iron-titanium oxides	4	0.5
Epidote	3	0.4
Prehnite	3	0.4
Spinel	2	0.3
Olivine	2	0.3
Sphene	1	0.1
Cement		
Iron-manganese oxide	297	39.6
Total	750	100.0

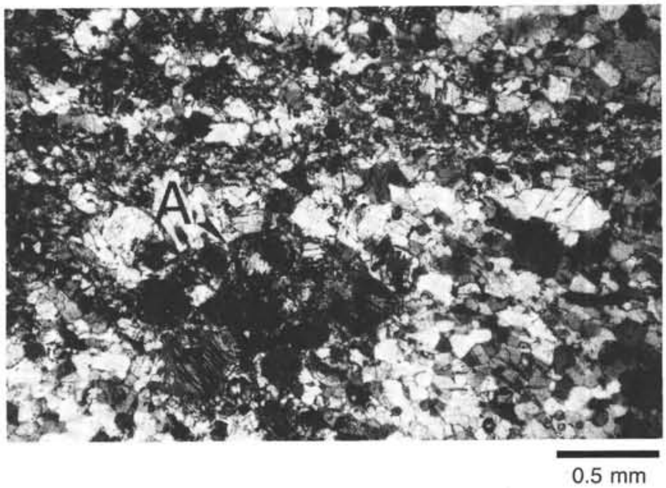

Figure 8. Foliated gabbro gneiss (Sample 118-732B-1D-2, 5-6 cm): recrystallized plagioclase and clinopyroxene (A). Crossed nicols.

temperature oxidative alteration, with clay minerals filling fractures and replacing phenocrysts or glassy mesostasis. In contrast, some of the basalts and all of the gabbroic samples show evidence of medium- to high-temperature metamorphism. In these rocks, the temperature of metamorphism appears related to the state of deformation: static metamorphism occurred at relatively low temperatures (stability of greenschist facies minerals), cataclastic deformation occurred at low to medium temperatures (stability of greenschist facies to low-amphibolite facies minerals), and plastic deformation occurred at still higher temperatures. Only three samples of peridotite were recovered, a mylonite and two coarse-grained harzburgites, all of which were heavily serpentinized.

Plastic Deformation of Gabbroic Rocks at High Temperature

One gabbro sample (118-732B-1D-2, 5-6 cm) shows a recrystallized and foliated texture (Fig. 8) with plagioclase neoblasts (mean size = 0.15 mm) and clinopyroxene grains that are 0.2 to 0.6 mm in size, surrounded by inclusion-free clinopyroxene neoblasts (less than 0.2 mm in size) and by blebs of brown hornblende. This texture was attributed to deformation-induced recrystallization of the gabbroic minerals at high temperatures. Evidence of such high-temperature recrystallization and deformation was documented for one of the DSDP Leg 37 gabbros (Helmstaedt, 1977) and for the Romanche, Vema, and Garrett transform zones (Hebert et al., 1983; C. Mevel, unpubl. data; Cannat, unpubl. data). Such high temperatures of metamorphism require proximity to a magma chamber and thus may be characteristic of the early cooling history of plutonic rocks near the ridge axis.

The sample also shows evidence of about 20% static alteration at lower temperatures: the cores of the clinopyroxene crystals are altered to a cloudy mesh of magnetite, serpentine, and clay minerals (Fig. 9). The primary ilmenite is rimmed by or intergrown with chlorite; small ilmenite inclusions in the plagioclase are replaced by sphene and fine-grained secondary magnetite; and euhedral pyrite crystals occur as inclusions in the plagioclase. The sample also displays relatively large, blocky, serpentinized porphyroclasts (1 mm in size) that may be igneous orthopyroxene, based on the presence of clinopyroxene exsolution lamellae (Fig. 10). If this interpretation is correct, the original gabbro was geochemically evolved with cumulus orthopyroxene.

Figure 9. Foliated gabbro gneiss (Sample 118-732B-1D-2, 5-6 cm). Clinopyroxene crystals with cores altered to a mesh of magnetite, serpentine, and clays, caused by post-deformation static alteration. Plane light.

Medium-Temperature Metamorphism and Cataclastic Deformation

Three gabbro samples (118-732C-3D-1, 5-10 cm, 118-732C-3D-1, 15-18 cm, Piece 4; and 118-732C-3D-1, 20-23 cm) are cut by fractures, which, from one sample to the next, may be randomly oriented or roughly parallel. The clinopyroxene is partly to completely replaced by brown to green hornblende (Fig. 11). Near the fractures, these hornblende crystals are kinked and partly recrystallized, either into smaller grains of the same hornblende or into a more actinolitic amphibole (Fig. 12). This suggests that the cataclastic deformation occurred over a range of decreasing temperatures. The response of plagioclase to deformation is also characteristic of a decrease in temperature: it may be locally recrystallized (Fig. 11), but more commonly it is crushed, heavily veined, and replaced by a fine aggregate of actinolite, epidote, and chlorite.

The metamorphic textures in these rocks are quite complex. The original ilmenite is heavily altered, with relict grains containing anatase or rutile inclusions and surrounded by jackets of coarse sphene (Fig. 13). In Sample 118-732C-3D-1, 15-18 cm, a characteristic (coronitic) replacement pattern preserves the rela-

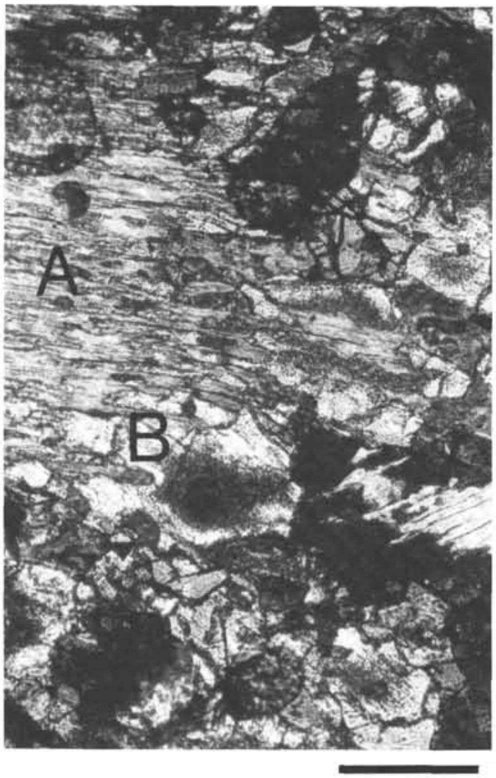

Figure 10. Foliated gabbro gneiss (Sample 118-732B-1D-2, 5–6 cm). Serpentinized porphyroclast (A) of what may be igneous orthopyroxene, based on the presence of clinopyroxene exsolution lamellae (B). Crossed nicols.

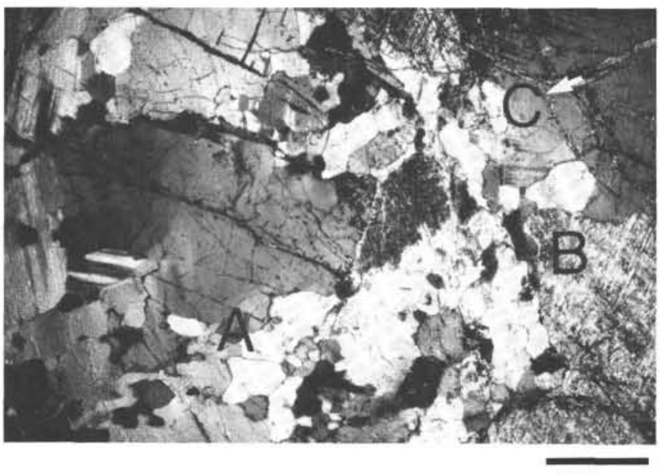

Figure 11. Recrystallized plagioclase (A), clinopyroxene partly altered to brown hornblende and actinolite (B) and a late chlorite vein (C). Gabbro Sample 118-732C-3D-1, 15–18 cm. Crossed nicols.

tionship of the primary minerals. As illustrated in Figure 14, plagioclase is replaced by chlorite, the boundary between plagioclase and the mafic phase is replaced by a colorless magnesian amphibole, and the core of the mafic phase is replaced by unidentified mineral dissected by rods of magnetite. The pseudo-

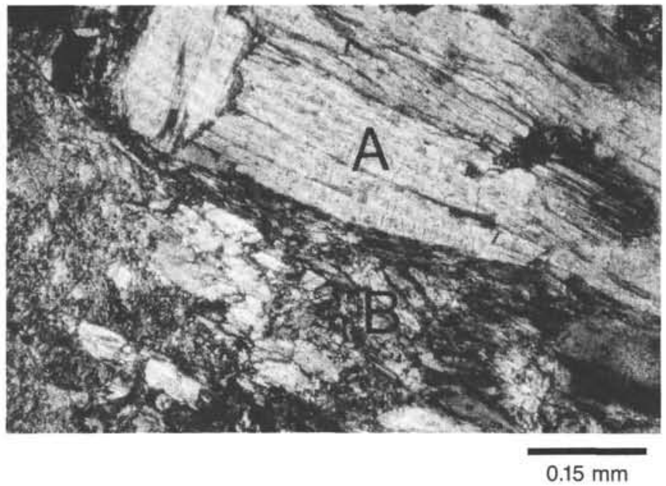

Figure 12. Green hornblende porphyroclast (A) recrystallized into margins of actinolitic porphyroblasts (B) in a zone of cataclastic deformation. Gabbro Sample 118-732C-3D-1, 20–23 cm. Crossed nicols.

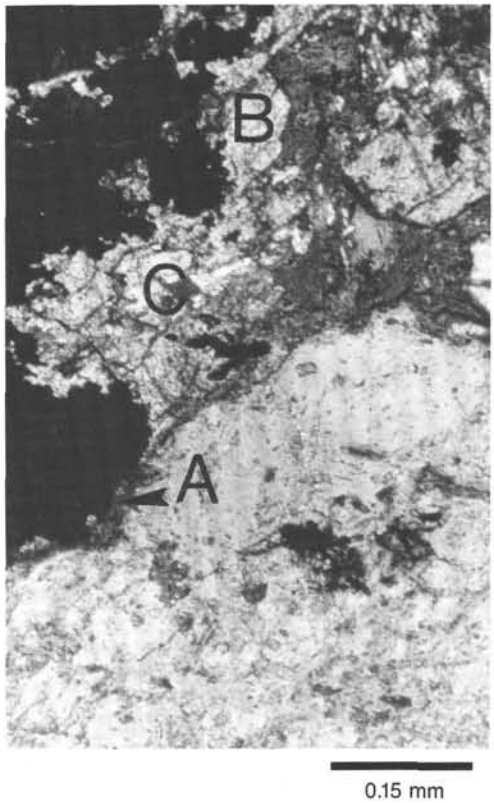

Figure 13. Primary igneous ilmenite (A) replaced by a jacket of coarse sphene (B) with one grain of included epidote (C). Gabbro Sample 118-732C-3D-1, 5–10 cm. Plane light.

morphed mafic phase may have been pyroxene because the magnetite rods in some of the grains appear to mimic cleavage planes. Veins of green hornblende, epidote (clinozoisite), and chlorite crosscut the foliation or the fractures. The magnetites are martitized, and most of the magnetite has been oxidized to hematite. A red vein sampled for XRD identification from Sam-

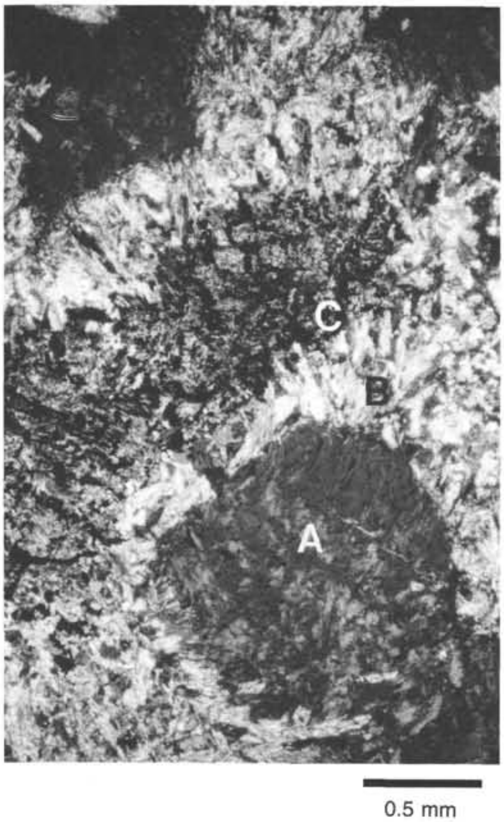

Figure 14. Metamorphic reaction rim in gabbro Sample 118-732C-3D-1, 15–18 cm. The surrounding plagioclase is replaced by chlorite (A). The boundary between plagioclase and the altered mafic phase (see text) is replaced by magnesian amphibole (B). The core of the mafic phase is replaced by unidentified mineral, dissected by rods of magnetite (C). Crossed nicols.

ple 118-732C-3D-1, 5–10 cm, proved to be a mixture of hematite and smectite.

Static Hydrothermal Alteration at Moderate Temperatures

Four pebbles of holocrystalline basalt (118-732B-1D-2, 6–7 cm; 118-732D-1D-1, 0–5 cm; 118-732D-1D-1, 21–25 cm; and 118-732E-1R-1, 17–20 cm) contain secondary chlorite, epidote, and actinolite. Chlorite replaces much of the plagioclase in these rocks and fills veins and vesicles. Epidote also fills veins and vesicles (Fig. 15) and replaces the cores of some of the plagioclase phenocrysts in Sample 118-732D-1D-1, 0–6 cm. Very thin veins of quartz (1–2 mm) that crosscut the basalt matrix have an *en-echelon* pattern resulting from shearing that is contemporaneous with quartz deposition. Much of the clinopyroxene in Sample 118-732B-1D-2, 6–7 cm, is replaced by epidote, whereas the plagioclase is replaced by acicular actinolite and lesser quantities of pale chlorite.

Of the plutonic rocks, one ferrogabbro (Sample 118-732D-1D-1, 7–8 cm) contains evidence of limited static metamorphism at moderate temperatures. In this sample, acicular actinolite replaces brown igneous hornblende and lesser quantities of plagioclase. The actinolite is itself partly replaced by brown smectite. In addition, serpentine-magnetite pseudomorphs replace either orthopyroxene or olivine. Large cumulus ilmenite phenocrysts have exsolved into two phases at temperatures equal to or greater than 600°C: a titanium-rich hematite and an iron-rich ilmenite. The phenocrysts also contain small, dark gray rods of

Figure 15. Greenschist facies altered basalt, Sample 118-732D-1D-1, 0–6 cm. An epidote-chlorite vein crosscuts the sample. Epidote and chlorite also fill the adjacent vesicle. Crossed nicols.

what may possibly be pleonaste. An included relict crystal of serpentinized olivine (?) contains both chalcopyrite and pyrite.

Finally, Sample 118-732B-1D-2, 9–10 cm, is a chip from a prehnite vein through a clinopyroxene- and orthopyroxene-bearing rock, probably a coarse-grained gabbro. The prehnite makes up about 90% of the sample and occurs as coarse, radial bundles (up to 3 mm wide) of bladed crystals. All the plagioclase apparently is replaced by prehnite, and the clinopyroxene is replaced by fine-grained actinolite and serpentine.

Low-Temperature Alteration

None of the samples contain any evidence of long exposure to seawater at low temperatures (i.e., seafloor weathering) since becoming a rubble fragment. There are no red oxidation rims on the pebbles, and clay minerals are not concentrated along the rounded margins of the samples. Instead, low-temperature mineral assemblages preferentially replace primary phases (e.g., glass replaced by green smectite). These observations suggest that the alteration and metamorphism occurred before the inclusion of the pebbles in the rubble. Most extrusive rocks contain clay minerals, some of which are stained with iron oxide. These clay minerals range from about 2% to 30% and replace both phenocrysts and groundmass and fill vesicles and fractures. Most are microcrystalline and probably smectite. Coarser aggregates of clay minerals appear to be green saponite or brown nontronite. No zonation of clay minerals was observed. Only trace amounts of other low-temperature minerals (zeolite and carbonate) occur in the vesicles. In one sample (118-732C-2D-1, 19–21 cm), olivine is replaced by calcite and some plagioclase may be replaced by potassium feldspar. This sample has a high K_2O content (see "Geochemistry" section, this chapter). Similar secondary mineral assemblages, observed in DSDP Holes 417A and 504B, were ascribed to low-temperature hydrothermal alteration under oxidative conditions (Scheidegger and Stakes, 1979; Pertsev and Boronikkin, 1983).

Ultramafic Rocks

Two very different ultramafic rocks were recovered at Site 732: a highly serpentinized, coarse-grained harzburgite (Samples 118-732B-1D-2, 8–9 cm, and 118-732D-1D-1, 8–9 cm) and a serpentinized peridotite mylonite (Sample 118-732A-1D-1, 0–4 cm). The coarse-grained harzburgite was plastically deformed under mantle conditions and shows a rough foliation marked by elongated orthopyroxene. Its subsequent serpentinization was static: a coarse mesh of serpentinite and magnetite replaces the olivine, and the pyroxenes are pseudomorphed by bastite. The spinel rims are replaced by magnetite. Chrysotile or lizardite veins having fibers perpendicular to the walls crosscut the samples.

The serpentinized peridotite mylonite is a strongly foliated rock composed mostly of serpentinite and magnetite. Magnetite is abundant (about 5%), varies greatly in size, and is distributed parallel to the foliation. A fine layering, parallel to the foliation, is defined by 1-mm-thick aggregates of actinolite or smectite mixed with the magnetite and fine-textured hematite (an oxidative alteration of the magnetite) in the serpentinite groundmass (Fig. 16). Rounded augen, composed of serpentinite and iron chromite enclosed in halos of green chlorite, appear to have been rotated in the foliation plane (Fig. 17), and the serpentinite foliation itself is locally deformed by microshear planes oblique to the foliation ("C"-type microshears; Berthe et al., 1979), with a dextral sense of offset in Figure 17. This type of microstructure is typical of a noncoaxial deformation regime.

The rounded shape of the augen and the very fine-grained texture of the serpentinite suggest that the rock was already a mylonite before serpentinization. The fine-grained serpentine replaced fine-grained mylonitized olivine, and the augen, now filled with serpentine and magnetite, may have been olivine or orthopyroxene porphyroclasts. The actinolite or smectite aggregates may be replacements of the original stretched orthopyroxenes or clinopyroxenes. If this hypothesis is correct, it implies that the deformation began at high temperatures, produced a peridotite mylonite, and continued at lower temperatures during the serpentinization process.

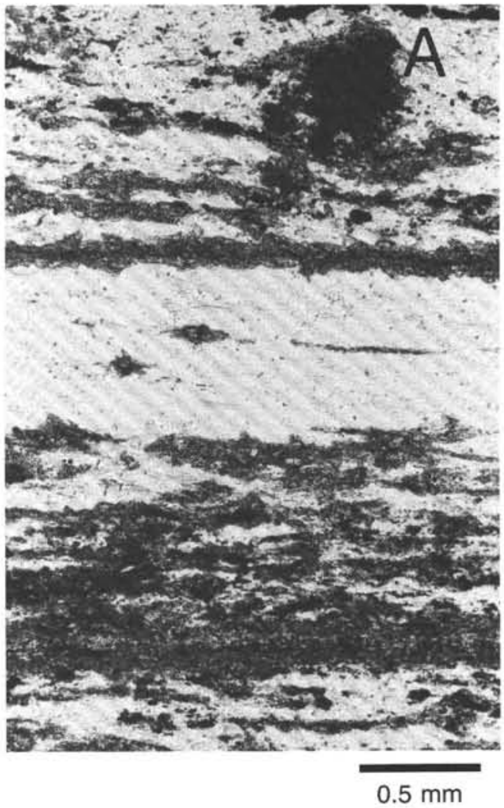

Figure 16. Serpentinized peridotite mylonite, Sample 118-732A-1D-1, 0–4 cm. The dark layers, parallel to the foliation, are composed of actinolite or smectite mixed with magnetite and hematitic alteration of the magnetite. The light layers are predominantly fine-grained serpentine. Also illustrated is a rounded augen of serpentinite and chromite (A). Plane light.

GEOCHEMISTRY

Five samples were analyzed for major and trace elements using the shipboard XRF system. The method is outlined in the "Introduction and Explanatory Notes" (this volume).

The analyzed samples include two aphyric basalts, one plagioclase-phyric basalt, one diabase, and one pyroxene gabbro. Results are summarized in Table 4. The weight loss on ignition (LOI) was determined gravimetrically; it reflects both loss of volatiles and uptake of oxygen from oxidation of ferrous iron during ignition. The relatively high LOI values for most samples attest to the presence of abundant secondary hydroxyl-bearing minerals.

The basalts are moderately fractionated, have magnesium numbers between 61 and 67, and contain less than 100 ppm of nickel. Nevertheless, these basalts rank among the least fractionated ones recovered from the Atlantis II Fracture Zone, as illustrated in Figure 18. The relatively high TiO_2, MnO, Na_2O, and P_2O_5 contents are in keeping with data for basalts dredged from the Southwest Indian Ridge (le Roex et al., 1983; Snow et al., in press). While the high potassium content of Sample 118-732C-2D-1, 21–23 cm, presumably results from low-temperature seawater alteration, the potassium content of the other samples is within the range of fresh Atlantis II Fracture Zone glasses analyzed by Snow et al. However, rubidium contents of the Site 732 samples are 1 to 3 ppm higher than for the Atlantis II Fracture Zone glasses, which implies that most of the samples have taken up rubidium during alteration. Diabase Sample 118-732D-1D-1, 20–25 cm, is more fractionated than the basalt (e.g., lower magnesium number, nickel, and chromium) and has the composition of an iron-titanium basalt.

The four basalts (including the diabase) from Site 732 are characterized by high zirconium/niobium (>32) and yttrium/niobium (≥8.6) ratios and clearly correspond chemically to the group of "depleted"-N-type, ocean-floor basalts that le Roex et al. (1983) found to be an ubiquitous lava type that erupted along the western end of the Southwest Indian Ridge between the Bouvet triple junction and 11°E. For example, this is illustrated by the yttrium vs. zirconium and niobium vs. zirconium diagrams shown in Figure 19 and confirmed by shore-based instrumental neutron-activation analyses of Samples 118-732C-2D-1, 12–15 cm, and 118-732D-1D-1, 20–25 cm, performed immediately after the cruise at the University of Leuven.

The consistently high abundances of incompatible elements such as titanium, zirconium, niobium, and yttrium in basalts derived from depleted sources are a strong indication that Atlantis II Fracture Zone basalts were formed by small degrees of partial melting, as predicted by recent tectono-magmatic models for fracture zones (e.g., Fox and Gallo, 1984).

The chemistry of pyroxene gabbro Sample 118-732C-3D-1, 20–23 cm, does not correspond to mid-ocean ridge basalt liquid compositions. The high chromium and strontium contents, coupled with low concentrations of titanium, vanadium, yttrium, zirconium, and niobium, indicate that this rock is a clinopyroxene plus plagioclase cumulate.

SUMMARY AND CONCLUSIONS

Site 732 is located on the median tectonic ridge of the Atlantis II Fracture Zone between 32°32.81′S, 57°03.289′E and 32°32.85′S, 57°02.7′E. This site was selected as the primary target for a deep reentry hole in upper mantle peridotite. Serpentinized peridotite was dredged from the median ridge during the site survey and was believed to crop out on the seafloor. The operational plan called for a television/sonar survey, a test spud-in at one or more favorable locations, setting of the hard-

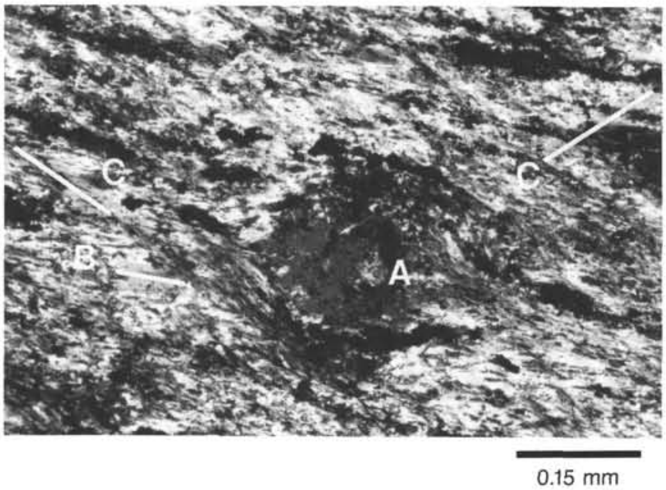

Figure 17. Rotated serpentine and iron chromite augen having green chlorite pressure-shadows (A) that indicate dextral shear. Note that the serpentinite foliation (B) is deformed by oblique microshear planes (C) having a dextral sense of offset. Crossed nicols.

rock guidebase, and drilling a 500+-m hole into basement. An extensive program of logging and downhole measurements was planned after completion of drilling.

Upon arrival at the site, an E-shaped television/sonar survey was conducted along the crest of the ridge, with three transects extending down the west flank. The surveys revealed blocky and bouldery outcrops on steep slopes on the flanks of the ridge and a rubbly, sedimented surface on the top of the ridge. Two sites on the crest of the ridge were selected for test spud-in in areas topographically suitable for guidebase deployment.

Six holes were drilled at Site 732, three each in the two different locations on the ridge crest. The deepest hole reached 24 mbsf. A total of 3.51 m of core material was obtained for an average recovery of 5.1%. These materials consist entirely of lithic granules, pebbles and cobbles, indurated sandstone, poorly consolidated sand, and muddy siliceous ooze. Drilling indicated that each hole penetrated a few (2-8) meters of soft sediment overlying a harder unit. Thus, it is likely that two lithologic units are present on the ridge crest: an upper layer of soft, muddy, siliceous ooze and a lower layer of gravel or conglomerate composed of igneous and metamorphic rock fragments containing interlayered sand and sandstone.

Calcareous nannofossils in the muddy siliceous ooze were tentatively assigned to Zone NN20 and dated as mid-Pleistocene, probably between 0.27 and 0.46 Ma (minimum 0.08, maximum 1.45 Ma). Sparse Oligocene to Pliocene species in the sediments suggest significant reworking and/or slumping at this site.

The lithic sandstone recovered at Site 732 consists primarily of basalt and diabase fragments and plagioclase, with lesser amounts of chlorite, amphibole, and clay minerals cemented by iron and manganese oxides.

The recovered clasts of igneous and metamorphic rock include basalt, diabase, gabbro, and minor serpentinized ultramafic rocks. Among the basalt clasts, aphyric and plagioclase-phyric varieties predominate. Sparse olivine phenocrysts or microphenocrysts are also present in three specimens. All of the basalts have quench textures, but no glass was recovered. Small, sparse vesicles, filled with chlorite or smectite, are present in two samples. Alteration is variable, while plagioclase is partly replaced by clay minerals, calcite, and chlorite; olivine is replaced by clay minerals, calcite, and chlorite; and interstitial

Table 4. Chemical data for Site 732 samples.

Hole	732C	723C	732C	732D	732F
Section	2D-1	2D-1	3D-1	1D-1	1R-1
Interval (cm)	12-15	21-23	20-23	20-25	31-34
Piece no.	3	4	5	4	7
Rock type	PB	AB	GA	DI	AB
(in wt%)					
SiO_2	49.88	51.62	50.10	49.84	50.16
TiO_2	1.87	1.75	0.47	2.10	1.50
Al_2O_3	17.77	17.04	14.52	14.79	15.91
Fe_2O_3	9.17	8.15	10.15	12.14	9.96
MnO	0.15	0.25	0.16	0.19	0.16
MgO	6.39	6.07	9.91	7.16	8.36
CaO	11.39	10.91	12.86	10.23	11.14
Na_2O	2.98	3.41	1.56	3.26	2.60
K_2O	0.17	0.60	0.25	0.11	0.07
P_2O_5	0.22	0.20	0.02	0.18	0.15
LOI	2.62	1.39	1.97	1.80	0.15
(in ppm)					
V	274	265	191	286	246
Cr	238	352	833	159	314
Ni	84	98	106	59	86
Cu	43	73	14	67	63
Zn	123	97	53	83	76
Rb	4	5	3	5	1
Sr	162	182	234	151	188
Y	43	41	22	38	31
Zr	156	148	61	142	119
Nb	4.3	4.3	2.4	4.4	3.4
Ratios					
Mg no. (× 100)	61.9	63.4	69.5	57.9	66.2
Ca no. (× 100)	67.9	63.9	82.0	63.5	70.3
K/Rb	350	1000	700	180	600
K/Sr	8.6	27.5	9.0	6.0	3.2
Zr/Nb	36.3	34.4	25.4	32.3	35.0
Zr/Y	3.62	3.61	1.41	3.74	3.84
Y/Nb	10	9.5	9.2	8.6	9.1

Major element data on anhydrous basis and normalized to sum = 100%. PB = plagioclase phyric basalt; AB = aphyric basalt; GA = gabbro; DI = diabase. LOI = loss on ignition. MG no. = $(Mg/Mg + 0.85\ Fe_{tot})_{molar}$; Ca no. = $(Ca/Ca + Na)_{molar}$.

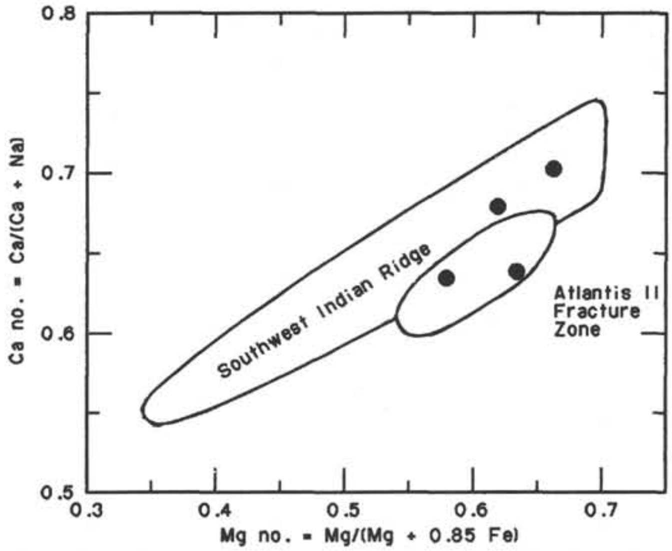

Figure 18. Calcium-number vs. magnesium-number for Site 732 basalts. Southwest Indian Ridge dredged basalt data from le Roex et al. (1983); Atlantis II Fracture Zone glass data from Snow et al. (in press).

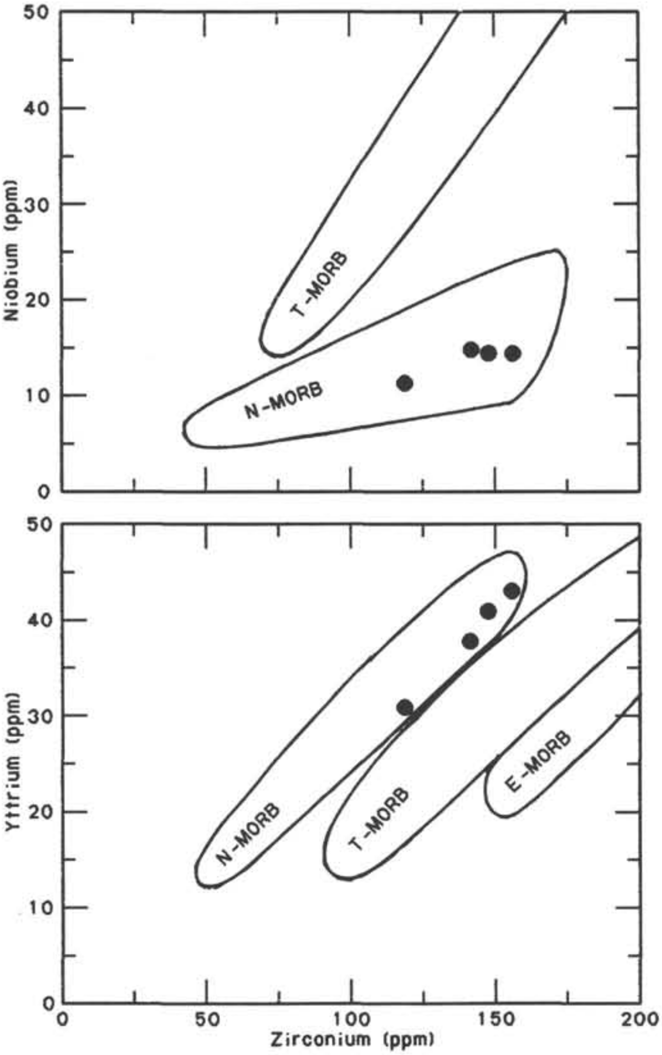

Figure 19. Zirconium, niobium, and yttrium contents of Site 732 basalts. Fields for Southwest Indian Ridge-dredged basalts from le Roex et al. (1983). The Site 732 basalts fall within the field of depleted normal Mid-Ocean Ridge (N-MORB) basalts. T-MORB = Transitional Mid-Ocean Ridge basalts. E-MORB = Enriched Mid-Ocean Ridge basalts.

material is replaced by clay minerals and chlorite. The diabase samples are mineralogically similar to the basalts but are somewhat coarser-grained.

Gabbro clasts range from moderately to highly altered and deformed, and from massive to foliated. Most consist of one-pyroxene gabbro, but a ferrogabbro may have originally had both orthopyroxene and clinopyroxene. One gabbro sample shows plastic deformation and high-temperature recrystallization with neoblasts of plagioclase and clinopyroxene. Medium-temperature alteration of other samples is manifested by replacement of the pyroxene by amphibole and by some cataclastic deformation. The ferrogabbro sample was subjected to static metamorphism at high to moderate temperatures, as manifested by actinolite replacing brown amphibole and serpentine-magnetite assemblages replacing either orthopyroxene or olivine.

Three pieces of ultramafic rock were recovered: two pieces of highly serpentinized, foliated harzburgite and one piece of serpentinized peridotite mylonite. In all cases, the serpentinization was probably static.

From the television/sonar survey, drilling operations, and recovered core material, the median tectonic ridge appears to be underlain by massive rock (peridotite?) and to be capped by a layer of poorly sorted breccia with interlayered sandstone. This sequence is overlain by a thin (2–8 m) layer of muddy siliceous ooze. We do not know exactly how thick the breccia layer is, but it is more than 20 m at Site 732. Clasts from the breccias are similar in size and composition to those recovered during the site survey from gravels on the floor of the transform farther south. These deposits were probably laid down by debris flows and turbidity currents originating on the steep walls of the transform. The appearance of these basinal sediments on top of the median ridge suggests uplift of that feature either by faulting or by serpentinite diapirism. Based on the age of the sediments, the uplift probably occurred after mid-Pleistocene time, which is probably only a small fraction of the transform age (~ 20 Ma). The inferred rates of uplift of the ridge are in the range of 0.3 to 0.5 cm/yr^{-1}, assuming that the ~ 1.5 km excess elevation of the ridge was created by continuous uplift from inception to the present day.

REFERENCES

Berthe, D., Choukroune, P., and Jegouzo, P., 1979. Orthogneiss, mylonite and noncoaxial deformation of granites: the example of the South Azmocican Shear Zone. *J. Struct. Geol.*, 1, 31–42.

Cormier, M.-H., Detrick, R. S., and Purdy, G. M., 1984. Anomalously thin crust in oceanic fracture zones: new seismic constraints from the Kane Fracture Zone. *J. Geophys. Res.*, 89:10249–10266.

Detrick, R. S., and Purdy, G. M., 1980. The crustal structure of the Kane Fracture Zone from seismic refraction studies. *J. Geophys. Res.*, 85:3759–3777.

Fox, P. J., Detrick, R. S., and Purdy, G. M., 1980. Evidence for crustal thinning near fracture zones: implications for ophiolites. *In* Panayioutou, A. (Ed.), *Proc. Int. Ophiolite Symp.* Ministry of Agriculture and Natural Resources, Cyprus Geol. Survey Dept., 161–168.

Fox, P. J., and Gallo, D. G., 1984. A tectonic model for Ridge-Transform-Ridge plate boundaries: implications for the structure of oceanic lithosphere. *Tectonophysics*, 104:205–242.

Hebert, R., Bideau, D., and Hekinian, R., 1983. Ultramafic and mafic rocks from the Garret transform fault near 13°30′S on the East Pacific Rise: igneous petrology. *Earth Planet. Sci. Lett.*, 65:107–125.

Helmstaedt, H., 1977. Postmagmatic textures and fabrics of gabbros and peridotites from DSDP Site 334. *In* Aumento, F., Melson, W. G., et al., *Init. Repts. DSDP*, 37: Washington (U.S. Govt. Printing Office), 763–774.

le Roex, A. P., Dick, H.J.B., Erlank, A. J., Reid, A. M., Frey, F. A., and Hart, S. R., 1983. Geochemistry, mineralogy and petrogenesis of lavas erupted along the Southwest Indian Ridge between the Bouvet Triple Junction and 11 degrees east. *J. Petrol.*, 24:267–318.

Martini, E., 1971. Standard Tertiary and Quaternary calcareous nannoplankton zonation. *In* Farinacci, A. (Ed.), *Proc. 2nd Planktonic Conf.*, 2:739–785.

Perch-Nielsen, K., 1985. Cenozoic calcareous nannofossils. *In* Bolli, H. M., Saunders, J. B., and Perch-Nielsen, K. (Eds.), *Plankton Stratigraphy*: London (Cambridge Univ. Press), 427–554.

Pertsev, N. N., and Boronikkin, V. A., 1983. Secondary K-feldspar in basalts at DSDP Hole 504B and the problem of K-feldspathization in oceanic basalts. *In* Cann, J. R., Langseth, M. G., Honnorez, J., Von Herzen, R. P., White, S. M., et al., *Init. Repts. DSDP*, 69: Washington (U.S. Govt. Printing Office), 589–591.

Scheidegger, K. F., and Stakes, D. S., 1979. X-ray diffraction and chemical study of secondary minerals from Deep Sea Drilling Project Leg 51, Holes 417A and 417D. *In* Donnelly, T., Francheteau, J., Bryan, W., Robinson, P., Flower, M., Salisbury, M., et al., *Init. Repts. DSDP*, 51/52/53 (Pt. 2): Washington (U.S. Govt. Printing Office), 1253–1264.

Schouten, H., and Klitgord, K. D., 1982. The memory of the accreting plate boundary and the continuity of fracture zones. *Earth Planet. Sci. Lett.*, 59:255–266.

Snow, J., Dick, H., and Hart, S., (in press). Petrogenesis of transform domain basalts from the Atlantis II Fracture Zone, Southwest Indian Ridge.

Thierstein, H. R., Geitzenauer, K. R., Molfino, B., and Shackleton, N. J., 1977. Global synchroneity of late Quaternary coccolith datum levels: validation by oxygen isotopes. *Geology*, 5:400–404.

Warren, B. A., 1978. Bottom water transport through the Southwest Indian Ridge. *Deep-Sea Res.*, 25:315–321.

Ms 118A-104